Signal Processing and Renewable Energy
December 2021, (pp. 29-49)
ISSN: 2588-7327
eISSN: 2588-7335

Synchronous Generator Excitation System Controller Design Using Feedback Linearization and H-Infinity Methods

Ebrahim Mohagheghian[1,2], Ghazanfar Shahgholian*[1,2], Bahador Fani[1,2]

[1] Department of Electrical Engineering, Najafabad Branch, Islamic Azad University, Najafabad, Iran.
[2] Smart Microgrid Research Center, Najafabad Branch, Islamic Azad University, Najafabad, Iran.

Received: 17-Jun-2021, Revised: 23-Jul-2021, Accepted: 25-Jul-2021.

Abstract

The power system stabilizer (PSS) is capable of improving network stability by damping oscillations. PSSs generate control signals for exciting system which are used to damp volatility resulting from impairment of the power system. To overcome the shortcomings of the conventional power system stabilizers by the use of feedback linearization control (FBLC) and H-infinity (H_∞) robust optimal control, two synchronous generator exciting system controllers were designed. The main objective is to design these controls to adjust the voltage and improve the stability of the power system small signal simultaneously despite uncertainty and disruptions to enter the power system. The simulation results obtained by MATLAB in a single machine to infinite bus (SMIB) system show that control proper functioning in different operational conditions, and are designed to be an appropriate alternative to conventional with automatic voltage regulator (AVR).

Keywords: FBL Control, H∞ Control, Power System Stabilizer, Small Signal Oscillations, Small Signal Stabilization.

1. INTRODUCTION

Security of the rotor angle stability and generator voltage regulation after the signal abnormalities even a small one, are intended as two important factors in determining the power system [1,2]. For this reason, a conventional power system is equipped with AVR to regulate generator voltage and provide security of the power system stability, and also it is equipped with power system stabilizer (PSS) [3,4].

PSSs are used in these large interconnected systems for damping out low-

*Corresponding Authors Email: shahgholian@iaun.ac.ir

frequency oscillations by providing auxiliary control signals to the generator excitation input [5,6].

But there are two problems with AVR+PSS conventional design [7,8]:

(a) The conventional AVR and PSS are designed separately, while the two strategies are applied simultaneously through the field voltage. As a result, simultaneous access to goals through voltage setting and stability securement is not possible.

(b) The performance of the conventional AVR+PSS is strongly dependent on the system operating point and in case of a significant deviation from the operating point, its performance is greatly weakened.

To overcome the above problems, the feedback linearization control (FBLC) has been extensively applied for the design of the synchronous generator exciting system so far [9,10]. In this method, the designer first defines a controlling law with one or several specific goals [11,12]. Voltage regulation and securement of the rotor angle stability are of the most important goals of control, but only the damping of the rotor angular oscillations after the occurrence of disturbances has been the goal of the designer in the initial designs; for this reason, these controllers play a weak performance in voltage regulation [13,14].

An exciting system controller in a FBL method is presented in [15] performing simultaneous voltage regulation and power system stabilization after small signal disturbances, but by an increase in the reactance of the transmission line, the damping torque applied to the power system by this controller is reduced and by its increase from a definite value, the power system will be unstable. Another controller in [16] is designed by FBL method. Since the q axis current can have a very small value in low frequency oscillations, the exciting field voltage will get larger which is considered a basic problem for this controller.

A new control law is presented in this paper in which the problem of the existence of i_q current in the control law denominator is solved. Also, this control law can properly damp the small signal oscillations within an extensive range of the power system operating conditions. One of the methods presented so far for the solution of the conventional PSS+AVR problems, is the H∞ resistance optimal control. The H∞ method is presented for the stable design of the power system in many references like [17,18]. An example of this method is reviewed in [19]. The goal for the design of this stabilizer is to regulate the voltage and secure the power system stability simultaneously. In the design of this stabilizer, two first-order weighting functions are first designed by the normalized-coprime factorization (NCF) method for the improvement of the controller performance. Then, by the use of the power system third-order linear model and considering the weighting functions, a fifth-order stabilizer is designed. The problem of this design is an increase in the order of the power system and an increase in complexity due to the presence of weighting functions. Due to the weighted functions, it increases the design complexity of the power system. For this reason, the design performed by the H∞ method is in a manner that there is no need for higher than the first-order weighting functions in this paper. This fact prevents an increase in the order of the controller and the complexity of the power system.

The issues presented in this paper are classified as follows: In the second section of this paper, the employed power system model is explained. In the third section, the exciting system controller design performed by the FBL method is presented. In the fourth section, the exciting system controller design performed by H∞ method without the use of weighting functions is described. In the fifth and the sixth sections, the results of simulations and conclusion are presented, respectively.

2. POWER SYSTEM MODEL

Power system is a highly complex and nonlinear system [19,20]. The single-machine to infinite-bus (SMIB) power system configuration shown in Fig. 1 is considered for this study [21,22]. U_T and U_B are the terminal voltage of synchronous machine and infinite-bus voltage. E_F and U_R are the electrical field output voltage and reference voltage. The conventional third-order model of synchronous machine is described by the electromechanical swing equation and the generator internal voltage equation [23,24]. The dynamic of the generator can be expressed by the following differential equations [25,26]:

$$\frac{d}{dt}\delta = \omega_b(\omega_r - 1) \tag{1}$$

$$\frac{d}{dt}\omega_r = \frac{1}{J_M}[T_M - T_E - K_D(\omega_r - 1)] \tag{2}$$

$$\frac{d}{dt}E_q^{'} = \frac{1}{T_{do}^{'}}[E_F + \underbrace{(X_d^{'} - X_d)i_d - E_q^{'}}_{E_q}] \tag{3}$$

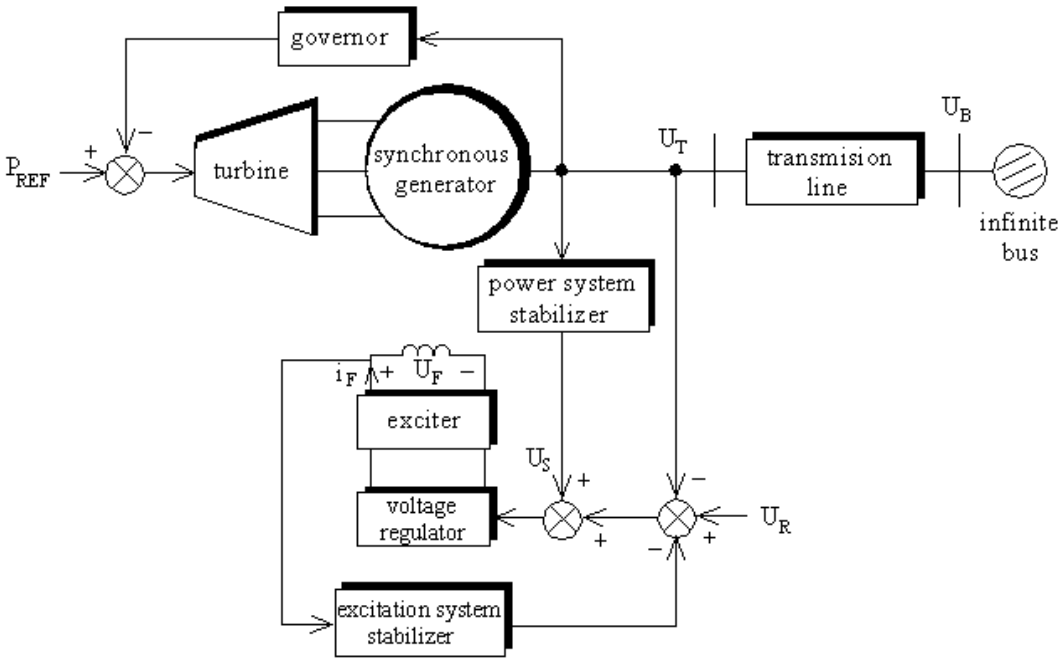

Fig. 1. Single-machine to infinite-bus power system.

where δ is angle load, J_M is the generator inertia constant, K_D is the inherent damping constant, ω_r is angular velocity, T_E is output electrical torque, T_M is input mechanical torque, E'_q is voltage proportional to direct axis flux linkages, X'_d is direct axis transient reactance, i_d is direct axis component of armature current, T'_{do} is the d-axis open circuit transient time constant, X_d is direct axis component reactance and ω_b is the base electrical angular velocity [27,28]. For AVR and PSS controllers, the most commonly used types are the IEEE type 1 for the AVR and the lead-lag-based structure for the PSS. However, other existing types could provide better results in terms of damping of power oscillations [29,30]. The electrical power delivered by a generator is given by [31]:

$$P_E = \frac{E'_q U_B}{X'_d + X_E} \sin\delta \tag{4}$$

The terminal voltage magnitude U_T can be expressed as:

$$U_T = \sqrt{\left(\frac{X_q U_B \sin\delta}{X_q + X_E}\right)^2 + \left(\frac{X'_d U_B \cos\delta + X_E E'_q}{X'_d + X_E}\right)^2} \tag{5}$$

The real power derivative and the voltage derivative of the synchronous generator bus required for the design of the controller through FBL method are as follows:

$$\begin{aligned} \frac{d}{dt}P_E &= \frac{U_B \sin\delta}{X'_d + X_E}\frac{d}{dt}E'_q + \frac{E'_q U_B \cos\delta}{X'_d + X_E}\frac{d}{dt}\delta(t) \\ &= \frac{U_B \sin\delta}{T'_{do}(X'_d + X_E)}(E_F + E_q) \\ &\quad + \frac{\omega_b E'_q U_B \cos\delta}{X'_d + X_E}\omega_r(t) \end{aligned} \tag{6}$$

$$\begin{aligned} &\frac{d}{dt}U_T \\ &= \underbrace{\left[\frac{-1}{U_T(\sin\delta)^2}\left[\frac{(P_E X_E)^2\cos\delta}{U_B^2\sin\delta} + \frac{X'_d X_E P_E}{X'_d + X_E}\right]\right]}_{f_1}\frac{d}{dt}\delta \\ &\quad + \underbrace{\left[\frac{1}{U_T\sin\delta}\left[\frac{P_E(X_E)^2}{U_B^2\sin\delta} + \frac{X'_d X_E\cos\delta}{X'_d + X_E}\right]\right]}_{f_2}\frac{d}{dt}P_E \end{aligned} \tag{7}$$

3. DESIGN OF THE EXCITING SYSTEM BY FBL METHOD

The following nonlinear control law is presented in [32] and [33] for the control of the synchronous generator exciting system:

$$\begin{aligned} E_F(t) = &\frac{1}{I_q(t)}\begin{bmatrix} v_f(t) \\ -T'_{do}\dfrac{E'_q(t)U_B\cos\delta(t)}{X_E + X_q}\omega_b\omega_r(t) \\ +P_M \end{bmatrix} \\ &+ (X_d - X'_d)I_d(t) \end{aligned} \tag{8}$$

where $v_f(t)$ is the control law input. The above equation is true for $I_q \neq 0$. The q axis current is negligible in low frequency oscillations. Since the q axis current is inserted in the denominator of the control law, the output of the control law or the very exciting field voltage during low frequency oscillations will be very large which is considered as a great drawback (defect, shortcoming) for the controller.

To remove this problem, a new control law is presented in this paper. To obtain the new control law, first a new input should be defined. There is no specific method to define the input and its selection is done

innovatively, but two points should be taken into consideration in selecting the input: 1- The defined input should be selected in a way that the nonlinear sections of the real power derivative and the voltage derivative of the generator bus are cancelled. 2- Since the control law is obtained by the solution of the input equation, the new input should be defined in a way that an optimal control law is ultimately obtained. The optimal control law is a law that can provide the required damping torque for the power system within a wide range of working conditions and also the problem of the presence of Iq current in its denominator is removed. With regard to the two above points, a new input is defined as follows:

$$v_f = E_F(t) - E_q(t) + \frac{E_q^{'} U_B \cos\delta}{X_d^{'} + X_E}\omega_b \omega_r(t) \qquad (9)$$

With regard to the new input equation (9), the real power derivative and the voltage derivative of the generator bus can be rewritten as follows:

$$\frac{d}{dt}\dot{P_E}(t) = \frac{E_q^{'} U_B \omega_b \cos\delta}{X_d^{'} + X_E}\left(1 - \frac{I_q}{T_{do}^{'}}\right)\omega_r(t) + \frac{I_q}{T_{do}^{'}} v_f(t) = A\,\omega_r(t) + \frac{I_q}{T_{do}^{'}} v_f(t) \qquad (10)$$

$$\frac{d}{dt}U_T(t) = \left[f_1 + A f_2\left(1 - \left(\frac{I_q}{T_{do}^{'}}\right)\right)\right]\omega_r + \frac{f_2 I_q}{T_{do}^{'}} v_f(t) = B\,\omega_r(t) + \frac{f_2 I_q}{T_{do}^{'}} v_f(t) \qquad (11)$$

Equations dP_E/dt and dU_T/dt are linearized by the application of the new input and can be used in the linear control theory. By solving equation (9), the new control law is obtained as follows:

$$E_F(t) = v_f(t) + E_q(t) - \frac{E_q^{'} U_B \cos\delta}{X_d^{'} + X_E}\omega_b \omega_r(t) \qquad (12)$$

In the above equation, $v_f(t)$ is the control law input. To secure the internal stability of the input system, the control law is obtained by the use of the second-order linear regulator in this paper. To obtain the input of the control law by the use of the second-order linear regulator theory, the equations of system state should be first written. The state variables are selected with regard to the control objective. The state variables of the system can be defined according to the following two states:

1) Rotor angle, rotor angular speed, synchronous generator real power $X=[\delta,\omega_r,P_E]^T$.

2) Generator terminal voltage, rotor angular speed, synchronous generator real power $X=[U_T,\omega_r,P_E]^T$.

In the first state, the main goal of the controller is to secure the stability of the rotor angle with no attention to the voltage regulation. The system state spatial model is as follows:

$$\dot{X} = A_{FBL} X + B_{FBL} V_{f\delta} \qquad (13)$$

where X is vector of state variables. The system matrix (A_{FBL}), control vector of equations (B_{FBL}) and controller input ($V_{f\delta}$) are given by:

$$A_{FBL} = \begin{bmatrix} 0 & \omega_b & 0 \\ 0 & \frac{-K_D}{J_M} & \frac{-1}{J_M} \\ 0 & A & 0 \end{bmatrix} \qquad (14)$$

$$B_{FBL}=\begin{bmatrix}0\\0\\\dfrac{I_q}{T'_{do}}\end{bmatrix} \quad (15)$$

$$V_{f\delta}=K_{\delta s}\Delta\delta+K_{\omega s}\Delta\omega_r+K_{ps}\Delta P_E \quad (16)$$

To have access to optimal voltage regulations in the second state, the generator bus voltage is considered as one of the state variables instead of the rotor angle. In this state, the performance of the controller is better than that of the previous state. The system state spatial model will be as follows:

$$\dot{X}=A_{FBL}X+B_{FBL}V_{fV} \quad (17)$$

where:

$$A_{FBL}=\begin{bmatrix}0 & B & 0\\0 & \dfrac{-K_D}{J_M} & \dfrac{-1}{J_M}\\0 & A & 0\end{bmatrix} \quad (18)$$

$$B_{FBL}=\begin{bmatrix}\dfrac{I_q f_2}{T'_{do}}\\0\\\dfrac{I_q}{T'_{do}}\end{bmatrix} \quad (19)$$

$$V_{fV}=K_{vv}\Delta U_T+K_{\omega sv}\Delta\omega_r+K_{pv}\Delta P_E \quad (20)$$

In [34], the calculation of the input coefficients of the control law ($K_{\delta s}$, $K_{\omega s}$, K_{ps}) and (K_{vv}, $K_{\omega v}$, K_{pv}) using theory of the second order linear regulator has been presented in detail. The main goals in the first and second attitudes are improvement of the rotor angle stability and voltage regulation of the generator bus, respectively. The voltage regulation and stability improvement have conflict with each other inherently. The membership functions (19) are used for elimination of this inherent conflict and achievement of the transient stability and voltage regulation are given by [35]:

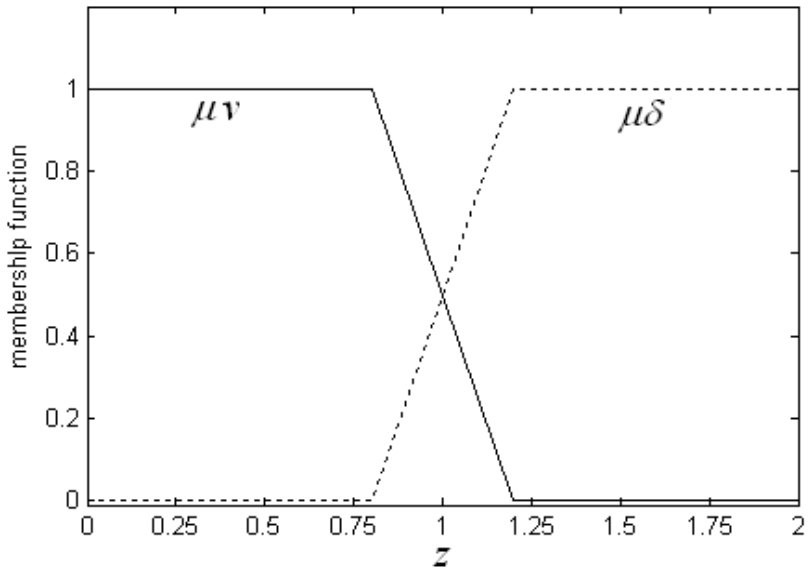

Fig. 2. Membership functions

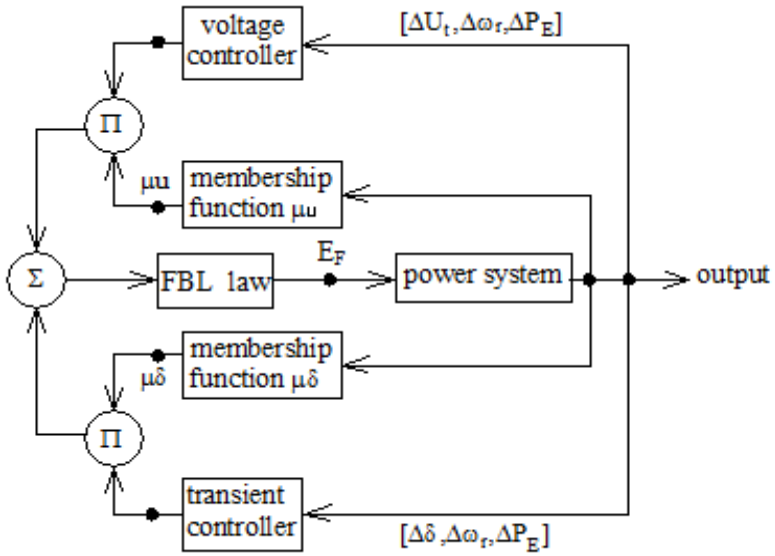

Fig. 2. Manner of the controller performance with the membership functions.

$$\mu v(z)=\left(1-\frac{1}{1+\exp(-120(z-1))}\right)\cdot\left(\frac{1}{1+\exp(-120(z+1))}\right) \quad (21)$$

$$\mu\delta(z)=1-\mu v(z) \quad (22)$$

$$z=\sqrt{\alpha_1(\Delta\omega)^2+\alpha_2(\Delta\delta)^2} \quad (23)$$

α_1 and α_2 are the positive and constant coefficients and they are chosen based on the goals of the design which are voltage regulation and improvement of the transient stability. Membership functions are shown in Fig. 2.

In this situation, the input of the control law is as follows:

$$\begin{aligned} V_f &= \mu_\delta \; V_{f\delta} + \mu_v V_{fv} \\ &= K_V\Delta V + K_\delta\Delta\delta + K_\omega\Delta\omega + K_p\Delta P \end{aligned} \quad (24)$$

The manner of operation of the excitation system controller has been shown in Fig. 3. The behavior of the controller which has been presented using membership functions is simply understandable considering Fig. 3.

4. CONTROL LAW APPLICATION IN PHILLIPS-HEFFRON MODEL

To apply the control law to the standard Phillips-Heffron model, the control law should first be linearized around the operating point. Then, all the variables should be rewritten in terms of the state variables of standard Phillips-Heffron model $(\omega, E'q, \delta)$ [36,37]. The linearized equation of the control law (16) is as follows:

$$\Delta E_F = V_f + \Delta E'_q + (X_d - X'_d)\Delta I_d - A\Delta\omega \quad (25)$$

The linearized Id is as follows [38]:

$$\Delta Id = Fd\,\Delta\delta + Yd\,\Delta E'q \quad (26)$$

By inserting equation (22) in (21), we can write:

$$\Delta E_F = \mathbf{V}_f + \Delta E'_q + \left(X_d - X'_d\right) Fd\,\Delta\delta + \left(X_d - X'_d\right) Yd\,\Delta E'q - A\,\Delta\omega \quad (27)$$

Now, the control law input, i.e. v_f should be inserted in equation (23):

$$\Delta E_F = -K_V \Delta V - K_\delta \Delta\delta - K_\omega \Delta\omega - K_p \Delta P + \Delta E'_q + \left(X_d - X'_d\right) Fd\,\Delta\delta + \left(X_d - X'_d\right) Yd\,\Delta E'q - A\,\Delta\omega \quad (28)$$

The voltage error can be defined as $\Delta V = \Delta Vt - \Delta Vref$. The linearized P and Vt are as follows:

$$\Delta P = K_1 \Delta\delta + K_2 E'_q \quad (29)$$

$$\Delta Vt = K_5 \Delta\delta + K_6 E'_q \quad (30)$$

With regard to the voltage error and equations (25) and (26), control law (24) can be rewritten as follows:

$$\Delta E_F = \mathbf{V}_f + \Delta E'_q + \left(X_d - X'_d\right) Fd\,\Delta\delta + \left(X_d - X'_d\right) Yd\,\Delta E'q - A\,\Delta\omega \quad (31)$$

$$\Delta E_F = K_{FBL}\left[-G5\,\Delta\delta - G6\,\Delta E'q + G_D\,\Delta\omega + \Delta V_{ref}\right] \quad (32)$$

where G_5, G_6 and G_D are given by:

$$G_5 = K_5 + \frac{K_\delta + K_p K_1 + \left(X_d - X'_d\right) F_d}{K_V}$$

$$G_6 = K_6 + \frac{1 + K_p K_2 + \left(X_d - X'_d\right) Y_d}{K_V}$$

$$G_D = \frac{-K_\omega - A}{K_V}$$

Fig. 4 shows the block diagram of equation (28). Fig. 4 is linear as the AVR block diagram, except that this block diagram includes an extra component of speed changes (Δω).

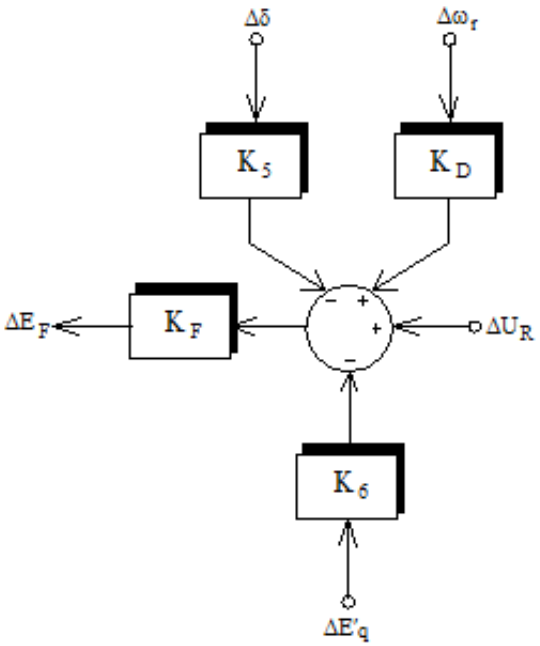

Fig. 3. Structure of the control system proposed on the basis of AVR.

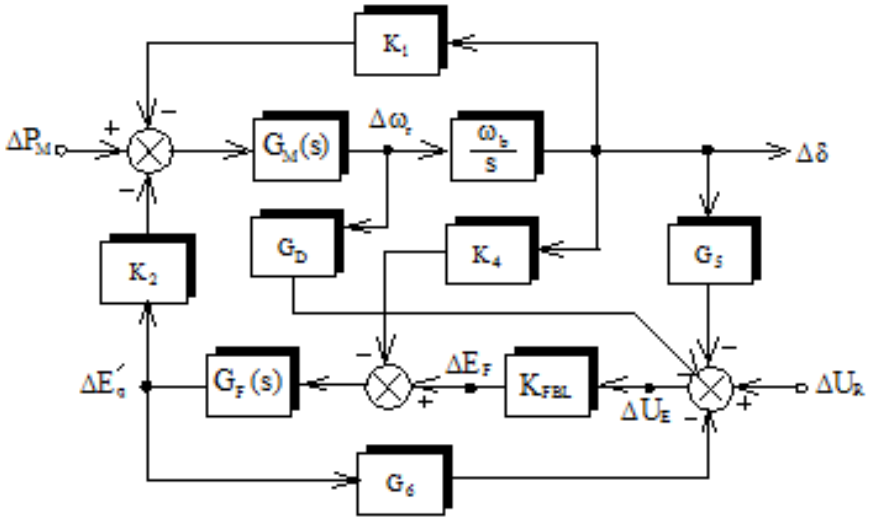

Fig. 4. Phillips-Heffron model consisting of linearized control law.

This extra component acts like a power system stabilizer and compensates the shortage of the system damping. This extra component is specified with a dotted circle. The proposed linear output feedback based on AVR can be interpreted as a fast-exciting system with a little time constant and KFBL gain. Two negative components affect the torque angle circle; the first from the rotor angular deviation $\Delta\delta$ shown with G5 gain and the second from the flux linkage deviation $\Delta E'_q$ shown with G6 gain. G5 and G6 are equal to K5 and K6 of standard Phillips-Heffron model. The SMIB block diagram along with the linearized control law is shown in Fig. 5.

5. EXCITING SYSTEM DESIGN BY H-INFINITY METHOD

A specific illustration of the system named the standard illustration is used in the H∞ standard problem. To solve a variety of problems brought up in the H∞control method, first these problems should be illustrated in a standard form. Standard illustration of H∞ controller and the manner of obtaining K(S) stabilizer controller are presented in references [39]. With the goal of simultaneous damping of the power system oscillations and regulation of the generator terminal voltage, a robust stabilizer is presented through the H∞ method. Fig. 6 shows the proposed standard H∞ controller.

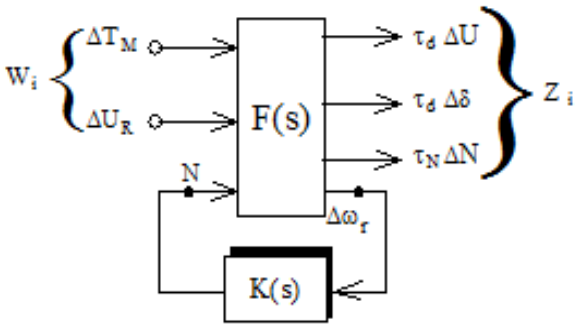

Fig. 5. The structure of the proposed H∞ controller.

With regard to this figure, the changes of ΔU_R reference voltage and those of the ΔT_M input torque are considered as the troublesome input or the very disturbance input.

To have access to simultaneous voltage regulation and improvement of rotor angle stability, the ΔV_t generator terminal voltage changes and those of $\Delta\delta$ rotor angle are selected by the application of suitable coefficients of η_v and η_δ as the regulated outputs. Also, by performing different simulations, it has been specified that if the feedback output is considered as one of the regulated outputs, the performance of the controller will be a lot better and more robust. The changes of $\Delta\omega_r$ rotor angular speed is either measured as the output or considered as the very input controller. The w_i disturbance input vector, the Z_i regulated output vector, and the Y measured output vector are considered as the following in this paper:

$$w_i^T = [\Delta T_M, \Delta U_R] \tag{33}$$

$$Z_i^T = [\eta_v \Delta V, \eta_\delta \Delta\delta, \eta_u \Delta U] \tag{34}$$

$$Y = \Delta\omega \tag{35}$$

The η_v, η_δ and η_u are constant weights selected by the designer with regard to the control goals.

The F(s) state space model of the proposed controller can be written as follows:

$$F(s):\begin{cases} \dot{X} = A\,x + B1\,w + B2\,u \\ Z = C1\,x + D11 w + D12\,u \\ Y = C2\,x + D21 w + D22\,u \end{cases}$$

$$\Rightarrow F(s) = \left[\begin{array}{c|c:c} A & B1 & B2 \\ \hline C1 & D11 & D12 \\ \hdashline C2 & D21 & D22 \end{array}\right] = \tag{36}$$

$$\left[\begin{array}{ccc:ccc} 0 & \omega & 0 & 0 & 0 & 1 \\ -\frac{K_1}{2H} & -\frac{D}{2H} & -\frac{K_2}{2H} & \frac{1}{2H} & 0 & 0 \\ -\frac{(k_4 + k_A K_5)}{T'_{do}} & 0 & \frac{(\frac{1}{K_3} + k_A K_6)}{T'_{do}} & 0 & \frac{K_A}{T'_{do}} & \frac{K_A}{T'_{do}} \\ \hline \eta_v K_5 & 0 & \eta_v K_6 & 0 & 0 & 0 \\ \eta_\delta & 0 & 0 & 0 & 0 & 0 \\ 0 & 0 & 0 & 0 & 0 & \eta u \\ \hdashline 0 & 1 & 0 & 0 & 0 & 0 \end{array}\right]$$

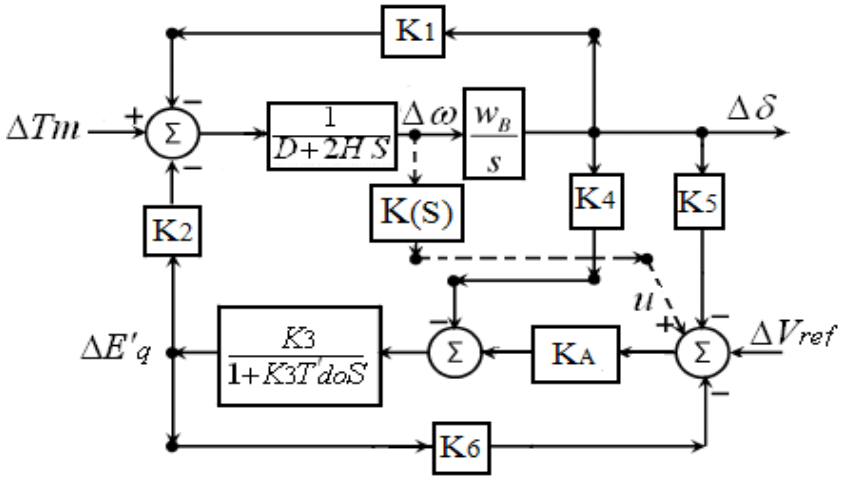

Fig. 6. The block diagram of the standard Phillips-Heffron model along with the H∞ robust stabilizer.

Table 1. ***Classification of the power system on the basis of the reactance of the transmission line.***

Transmission system	X_E(pu)
Weak	$X_E \geq 0.6$
Medium	$0.3 < X_E < 0.6$
Strong	$X_E \leq 0.3$

In the above state space model, A is the state space model of standard Phillips-Heffron model with the $X = [\Delta\delta, \Delta\omega, \Delta E'q]$ state vector. Also, u is the control input (stabilizer output signal). The block diagram of the standard Phillips-Heffron model along with H∞robust stabilizer are plotted in Fig. 7. In the H∞ method, the order of the controller is equal to that of the open-loop system in addition to the sum of the order of the weighting functions. Since the weighting functions in this design are of zero-order, the order of the presented stabilizer is equal to the number of the system state variables.

In this paper, the voltage automatic regulator dynamics is selected as the KA constant gain. In this method, contrary to the design of the conventional power system stabilizer, the AVR dynamics is taken into consideration and the K(S) is designed with regard to this dynamic; as a result, simultaneous regulation of the voltage and securement of stability is possible.

6. SIMULATION RESULTS

The transmission system can be divided into three systems of strong, medium, and weak with regard to the size of the impedance between the infinite bus and the (Xe) generator as shown in Table 1 [40].

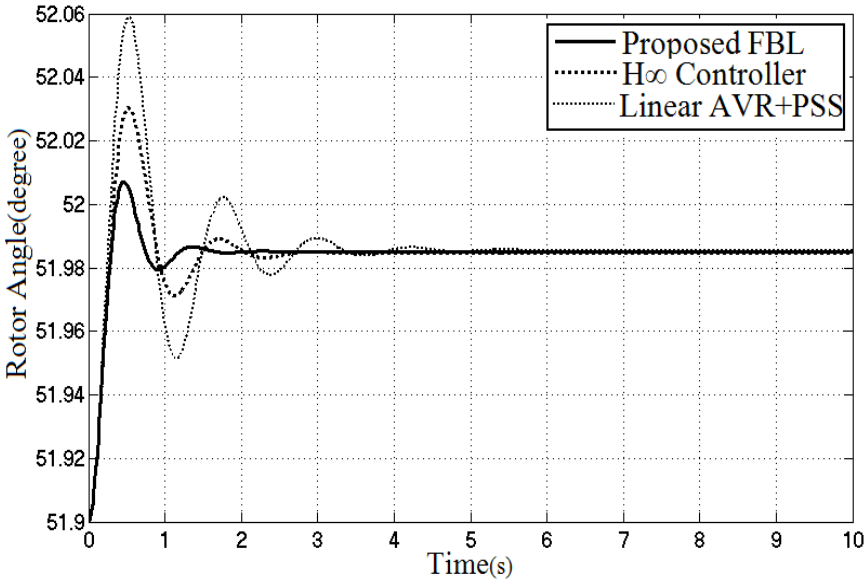

Fig. 7. Rotor angle changes, 10% change in the input torque, strong transmission system.

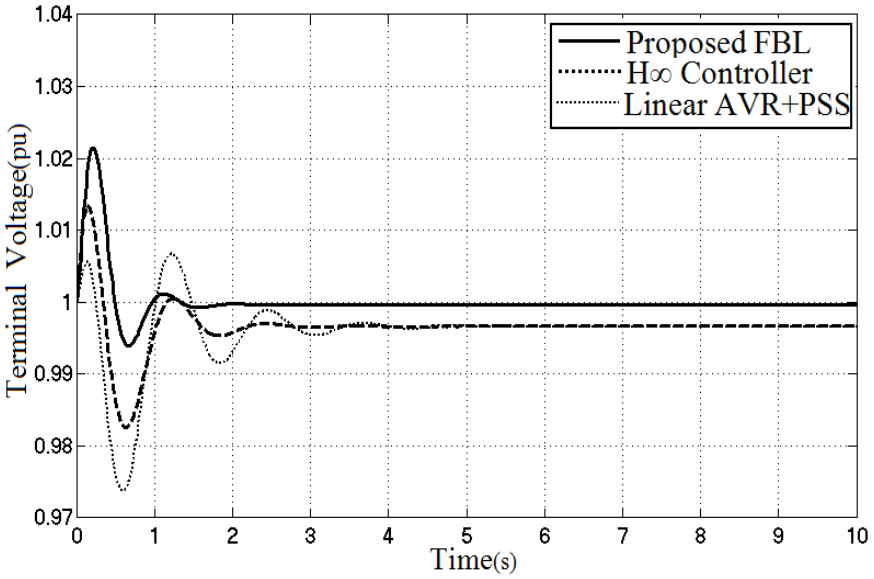

Fig. 8. Terminal voltage changes, 10% change in the input torque, strong transmission system.

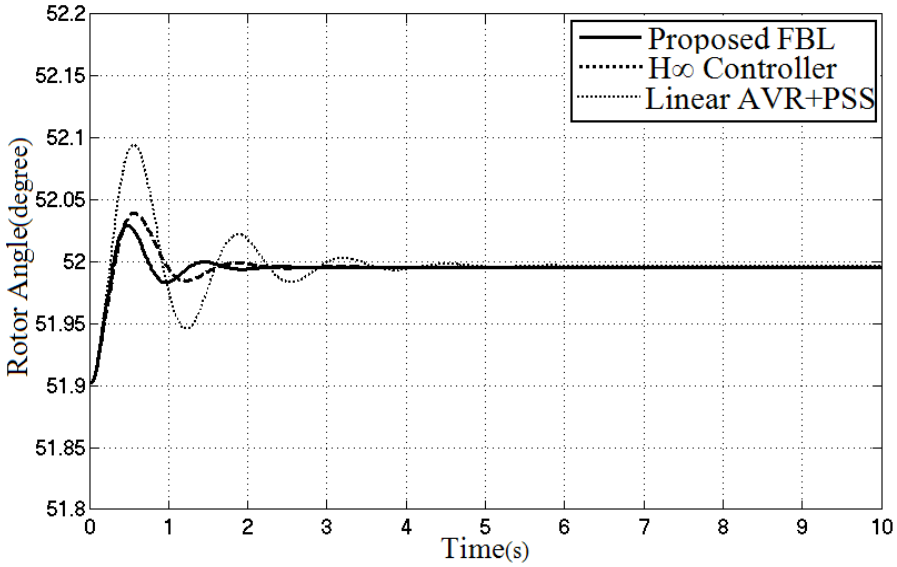

Fig. 9. Rotor angle changes, 10% change in the input torque, medium transmission system.

The type of the transmission system is considered as an important factor in the performance of the controllers. For example, a controller might have an acceptable performance under strong and medium transmission system, but in a state of a weak transmission system, its performance might be unacceptable. For this reason, to demonstrate that the controllers enjoy satisfactory performance under strong, medium, and weak transmission system conditions, the performance of these two controllers are studied under the three states of strong, medium, and weak transmission systems.

Figs. 8 and 9 illustrate the rotor angle changes and generator terminal voltage of the strong transmission system due to an increase

of the input torque by 10%. By the application of FBL controller, the amplitude of oscillations is less and they are damped faster and voltage regulation is more precise. With regard to Fig. 9, after the 10% change in the input torque, the voltage value of the generator bus with the FBL controller remains exactly at 1 pu, but the voltage drops with the other two controllers.

Figs. 10 and 11 show the medium system response. Fig. 10 shows the rotor angle changes due to a 10% reduction in the input torque and Fig. 11 shows the rotor terminal voltage due to a 10% increase in the reference voltage. In this state, the time duration required for the power system response to reach its final value is the same in the two proposed controllers. Also, as in the previous state, regulation of the FBL controller voltage is more precise.

In this state, the amplitude of oscillations of H∞ controller is less than that of the FBL controller, but it reaches its final value after about 2.5 seconds with the two power system controllers.

The interesting point to note is that the performance of the conventional AVR+PSS is very undesirable under weak transmission system.

The main uncertainty in a power system is related to the impedance change between the infinite bus and the generator. The most important factor of impedance change relates to the disconnection of the transmission line. The disconnection of transmission lines can cause the change of the system from one kind to another; for example, by the disconnection of one of the transmission lines in a medium system, Xe might get somewhat greater and the transmission system becomes weak. To study the rate of the resistance of the controllers proposed relative to the Xe parameter, their performance is studied after the disconnection of one of the transmission lines in the three states of transmission system.

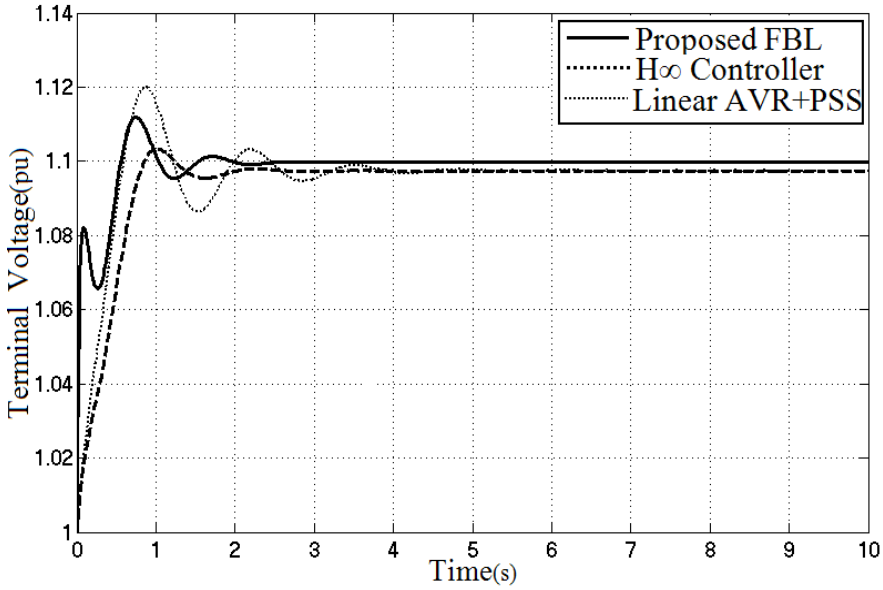

Fig. 10. Terminal voltage changes, 10% change in the input reference voltage.

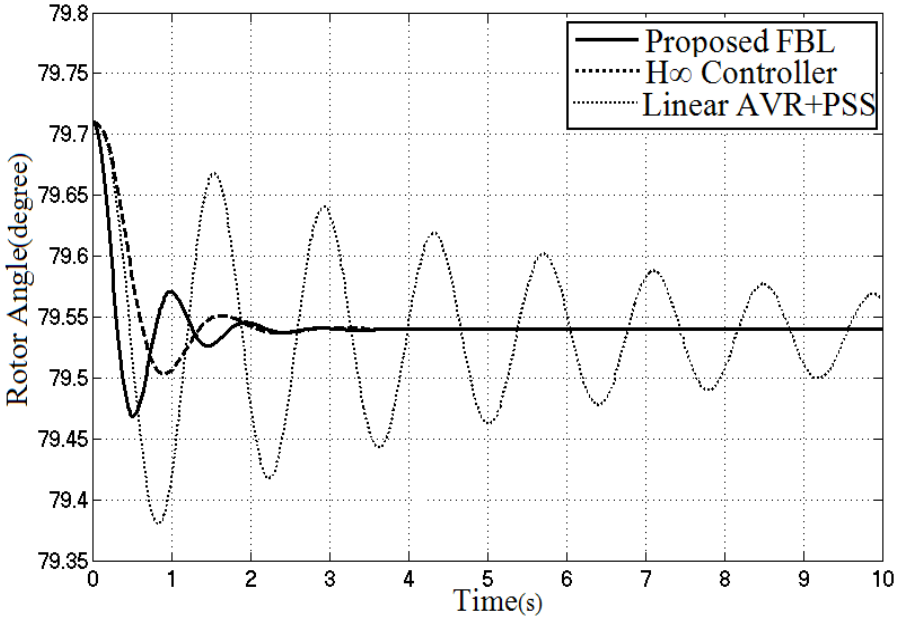

Fig. 11. Rotor angle changes, 10% change in the input reference voltage, weak transmission system.

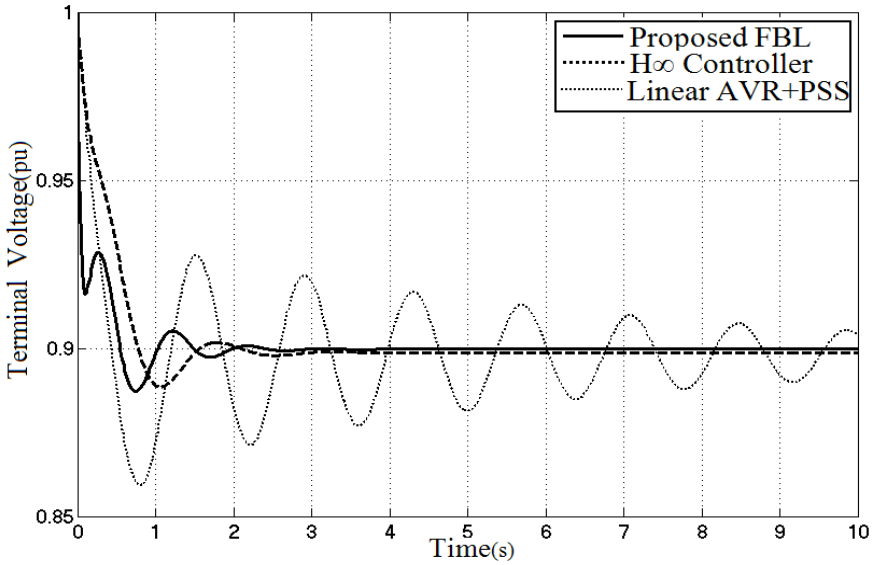

Fig. 12. Terminal voltage changes, change in the input reference voltage, weak transmission system.

With regard to Figs. 14 and 15, both FBL and H∞ controllers have somewhat similar performance in damping the voltage oscillations and the angel of the generator rotor connected to the strong and medium transmission systems, but still the FBL controller voltage regulation is better. With regard to Figs. 16 and 17, the performance of H∞ controller in damping oscillations is better than that of FBL controller in the state of weak transmission system, but in this state too, regulation of FBL controller voltage is more precise.

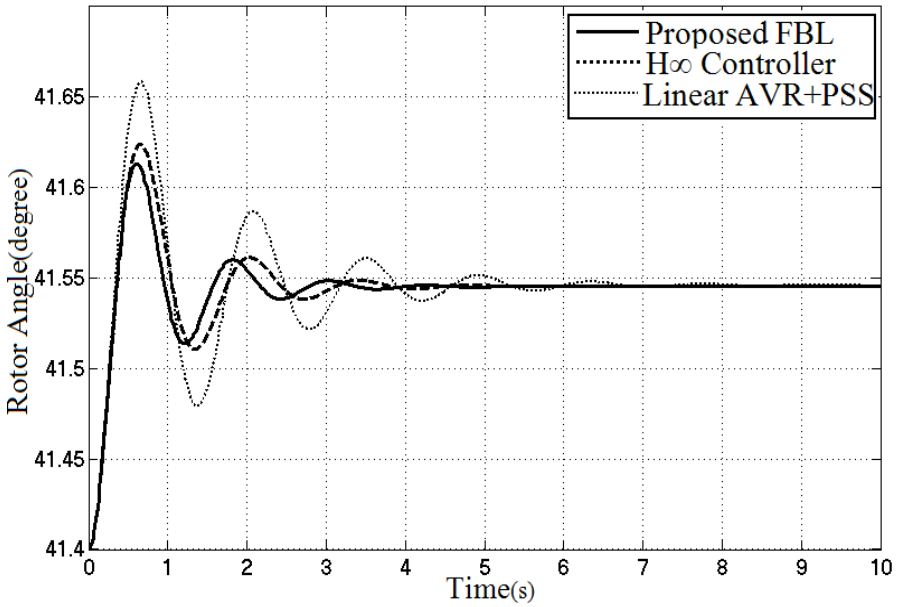

Fig. 13. Rotor angle changes, 10% change in the input torque, strong transmission system with the disconnection of one of the transmission lines.

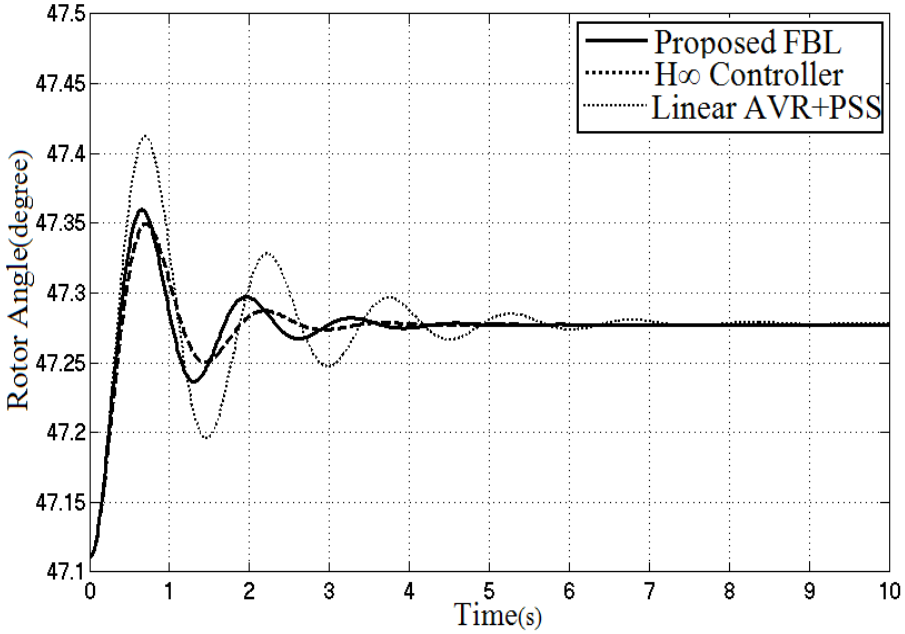

Fig. 14. Rotor angle changes, 10% change in the input torque, medium transmission system with the disconnection of one of the transmission lines.

For a closer study and better comparison of the performance of the proposed conventional AVR+PSS, FBL, and H∞ controllers, the analysis of the specific values is used. The system oscillation modes and damping coefficients at three operating points (appendix 3) are obtained for all the three types of the transmission system. Table

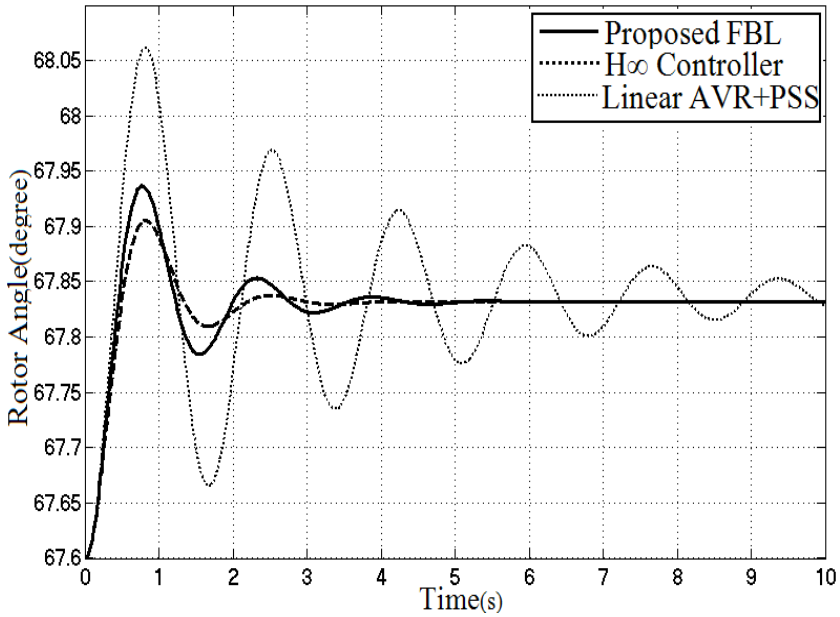

Fig. 15. Changes of the rotor angle, 10% change in input torque, weak transmission system with the disconnection of one of the transmission lines.

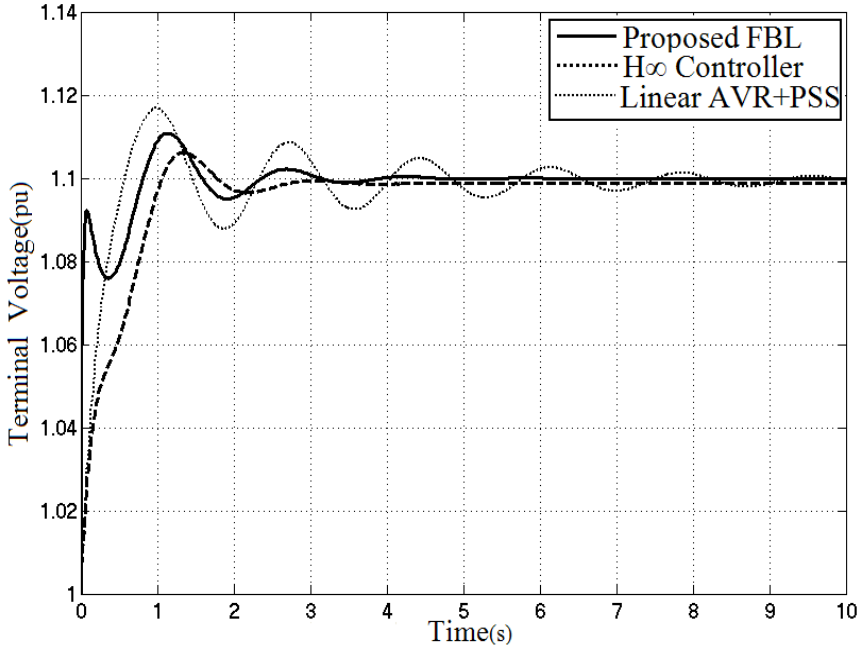

Fig. 16. Changes of the terminal voltage, 10% change in the input reference voltage, weak transmission system with the disconnection of one of the transmission lines.

2 shows these values for the ordinary transmission system and Table 3 presents them for the transmission system with the disconnection of one of the transmission lines.

In all the states, it is clear that the controllers presented have an ideal performance and have better performance relative to the conventional AVR+PSS. In a power system with the conventional AVR+PSS, the damping coefficient is significantly reduced by an increase in the transmission line reactance meaning a reduction in the damping torque applied to the power system. But, by an increase in the transmission line reactance in the proposed H∞ robust controller, the damping torque applied to the power system is increased showing the controller resistance to Xe. An increase in the reactance of the transmission line in FBL controller results in a decrease in the damping torque applied to the power system, but this reduction is not so great and brings about no problem for the controller. Only in the state of strong transmission system the damping torque applied to the power system by the FBL controller is more than that applied to the H∞ controller, but in the medium and weak transmission systems, the damping torque applied to the power system by the H∞ controller is more than that applied to the FBL controller. The performance of the two proposed controllers in damping the oscillations is relatively equal in the state of the medium transmission system, but in the state of the weak transmission system, the superiority of the H∞ robust controller in damping the oscillations of the power system is more evident than that of the FBL controller. The noticeable point is that in all the states, voltage regulation performed by the FBL controller is more precise than that performed by the other two controllers.

Table 2. ***Mechanical mode of oscillation modes and damping coefficients of the power system by the application of the exciting system controller.***

Controller	Stiff	Median	Weak
FBL	-2.92±j7.034 (38.34%)	-2.01±j6.45 (29.7%)	-1.4417±j5.63 (24.79%)
H_∞	-2.01±j5.45 (34.57%)	-2±j4.91 (37.72%)	-1.68±j4.35 (36.03%)
CPSS+AVR	-1.315±j5.16 (24.7%)	-0.99±j4.79 (20.31%)	-0.684.52 (3.7%)

Table 3. ***Mechanical mode of oscillation modes and damping coefficients of the power system by the disconnection of one of the transmission lines by the application of the exciting system controller.***

Controller	Stiff	Median	Weak
FBL	-1.2±j5.22 (22.35%)	-1.08±j4.87 (21.61%)	-1.01±j4.054 (20.34%)
H_∞	-1.14±j4.54 (24.35%)	-1.29±j4.21 (29.3%)	-1.35±j3.54 (32.82%)
CPSS+AVR	-0.7±j4.42 (15.68%)	-0.64±j4.13 (15%)	0.49±j3.57 (13%)

One of the important points in selecting the type of controllers is the complexity and the order of the controller. The H∞ controller is more complex compared to the two other controllers and its order is higher. The order of this controller is 3 and by applying it to the power system, the order of the system will increase to 6. The FBL controller does not increase the order of the system at all and with this controller the power system remains at order 3.

The conventional stabilizer of the power system is at least at order 2 and in complexity it is simpler than the H∞ robust controller. By the application of this controller to the power system, the order of the system converts to 5. It can be concluded that the FBL controller is much simpler than the other two controllers.

7. CONCLUTION

Two controllers for synchronous generator exciting system were designed and compared by FBL and H∞ methods in this paper. The use of the second-order linear regulator in FBL method results in the guaranty of the internal stability of the system; also, the use of the membership functions removes the inherent opposition between the voltage regulation and stability securement while the response of the system will be softer and better. The weighting functions were not used in the H∞ method for the design of the controller. This fact not only did not have a negative effect on the performance of the controller, but it also resulted in the reduction of the order of the controller and the power system. In all the states, the voltage regulation performed by the FBL controller is more precise than that performed by the H∞ controller. From the view of damping the power system oscillations with the strong transmission system, the performance of the FBL controller is better than that of the H∞ controller. In the state of the medium transmission system, the performance mean of the two controllers is almost similar and in the state of the weak transmission system, the H∞ controller performance is better than that of the FBL controller. The results of simulations and analysis of the specific values show that the new control law and the presented H∞ stabilizer are able to apply the required damping torque to the power system within a wide range of working conditions and regulate the generator bus voltage like a fast stimulator with small time constant. The most important uncertainties relate to the change in the operating point and also the uncertainties resulting from the disturbances; the presented controllers prove to have optimal performance against these uncertainties. The two proposed controllers have better performance than the conventional PSS+AVR within a wide range of power system working conditions and can be suitable replacement for it.

REFERENCES

[1] Batmani, Y., Golpîra, H., (2019). Automatic voltage regulator design using a modified adaptive optimal approach, International Journal of Electrical Power and Energy Systems, 104: 349-357.

[2] Fattollahi, A. (2017). Simultaneous design and simulation of synergetic

power system stabilizers and a thyristor-controller series capacitor in multi-machine power systems, Journal of Intelligent Procedures in Electrical Technology, 8 (30): 3-14.

[3] Fattollahi-Dehkordi, A., Shahgholian, G., Fani, B. (2020). Decentralized Synergistic Control of Multi-Machine Power System Using Power System Stabilizer. Signal Processing and Renewable Energy, 4(4): 1-21.

[4] Shahgholian, G., Movahedi, A., Faiz, J. (2015): Coordinated design of TCSC and PSS controllers using VURPSO and genetic algorithms for multi-machine power system stability. International Journal of Control, Automation, and Systems, 13(2): 398-409.

[5] Kumar, A. (2020): Nonlinear AVR for power system stabilisers robust phase compensation design. IET Generation, Transmission and Distribution, 14(21): 4927-4935.

[6] Zhang, G. et al. (2020): Deep reinforcement learning-based approach for proportional resonance power system stabilizer to prevent ultra-low-frequency oscillations. IEEE Trans. on Smart Grid, 11(6): 5260-5272.

[7] Lala, J. A. O., Gallardo, C. F. (2020): Adaptive tuning of power system stabilizer using a damping control strategy considering stochastic time delay. IEEE Access, 8: 124254-124264.

[8] Kundur, P. (1994). Power system stability and control, McGraw-Hill.

[9] Kazemi, A., Jahed-Motlagh, M. R., Naghshbandy, A. H. (2007). Application of a new multi-variable feedback linearization method for improvement of power systems transient stability. International Journal of Electrical Power and Energy Systems, 29(4): 322–328.

[10] Gurrala, G., Sen, I. (2011). A nonlinear voltage regulator with one tunable parameter for multimachine power systems, IEEE Trans. on Power Systems, 26(3): 1186-1195.

[11] Yuan, X., Chen, Z., Yuan, Y., Huang, Y., Li, X., Li, W. (2016). Sliding mode controller of hydraulic generator regulating system based on the input/output feedback linearization method, Mathematics and Computers in Simulation, 119: 18–34.

[12] Yuan, X., Chen, Z., Yuan, Y., Huang, Y., (2015). Design of fuzzy sliding mode controller for hydraulic turbine regulating system via input state feedback linearization method, Energy, 93(1): 173–187.

[13] Marino, R. (1984). An example of a nonlinear regulator. IEEE Trans. on Automatic Control, 29(3): 276-279.

[14] Shafiullah, M., Rana, M. J., Shahriar, M. S., Zahir, M. H. (2019). Low-frequency oscillation damping in the electric network through the optimal design of UPFC coordinated PSS employing MGGP, Measurement, 138: 118-131.

[15] Mak, F.K. (1992). Design of nonlinear generator exciters using differential geometric control theories, Proceeding of the IEEE/DC, 1: 1149-1153.

[16] Zhu, C., Zhou, R., Wang, Y. (1997). A

new nonlinear voltage controller for power systems, International Journal of Electrical Power and Energy Systems, 19(1): 19–27.

[17] Rosaline, A. D., Somarajan, U. (2019). Structured H-ınfinity controller for an uncertain deregulated power system. IEEE Trans. on Industry Applications, 55(1): 892-906.

[18] Yang, M., Li, Y., Du, H., Li, C., He, Z. (2019). Hierarchical multiobjective H-Infinity robust control design for wireless power transfer system using genetic algorithm". IEEE Trans. on Control Systems Technology. 27(4): 1753-1761.

[19] Senjyu, T., Morishima, Y., Yamashita, T., Uezato, K., Fujita, H. (2002). Decentralized H_∞ excitation controller achieving damping of power system oscillations and terminal voltage control for multi-machine power system, Proceeding of the IEEE/PES, 1: 174-179.

[20] Kazemi Zahrani, A., Parastegari, M. (2017). Designing PSS and SVC parameters simultaneously through the improved quantum algorithm in the multi-machine power system", Journal of Intelligent Procedures in Electrical Technology, 8(31): 68-75.

[21] Mahdavian, M., Behzadfar, N. (2020). A review of wind energy conversion system and application of various induction generators, Journal of Novel Researches on Electrical Power, 8(4): 55-66.

[22] Milla, F., Duarte-Mermoud, M.A. (2018). Predictive optimized adaptive PSS in a single machine infinite bus. ISA Transactions, 63: 315-327.

[23] Wan, Y., Jiang, B., (2015). Practical nonlinear excitation control for a single-machine infinite-bus power system based on a detailed model. Automatica, 62: 18-25.

[24] Alberto, L. F. C., Bretas, N. G. (2000). Application of Melnikov's method for computing heteroclinic orbits in a classical SMIB power system model, IEEE Trans. on Circuits and Systems I: Fundamental Theory and Applications, 47(7): 1085-1089.

[25] Yang, S., Zhang, B., Hojo, M., Su, F. (2018). An ME-SMIB based method for online transient stability assessment of a multi-area ınterconnected power system, IEEE Access, 6: 65874-65884.

[26] Fani, B., Mahdavian, M., Farazpey, S., Janghorbani, M., Azadeh, M. (2016). Improving dynamic stability of power system using derivative power system stabilizer. Proceeding of the IEEE/EC-TICON, Chiang Mai, Thailand, pp. 1-6.

[27] Ghasemi, M., Roosta, A., Fani, B. (2012). Coordinated control of FACTS devices by using ADALINE neural network to enhance the transient stability of power system. Journal of Intelligent Procedures in Electrical Technology, 3(9): 27-40.

[28] Essallah, S., Bouallegue, A., Khedher, A. (2019). Integration of automatic voltage regulator and power system stabilizer: small-signal stability in DFIG-based wind farms, Journal of Modern Power Systems and Clean Energy, 7(5): 1115–1128.

[29] Shahgholian, G., Movahedi, A. (2016). Power system stabiliser and flexible

alternating current transmission systems controller coordinated design using adaptive velocity update relaxation particle swarm optimisation algorithm in multi-machine power system, IET Generation, Transmission and Distribution, 10 (8): 1860-1868.

[30] Bhukya, J., Mahajan, V., (2019). Optimization of damping controller for PSS and SSSC to improve stability of interconnected system with DFIG based wind farm, International Journal of Electrical Power and Energy Systems, 108: 314-335.

[31] Liu, H., Su, J., Yang, Y., Qin, Z., Li, C. (2021). Compatible decentralized control of AVR and PSS for ımproving power system stability. IEEE Systems Journal, 15(2): 2410-2419.

[32] Jenab, S., Fani, B., Ghasvari, H. (2014). Transient performance ımprovement of wind turbines with doubly fed ınduction generators using fractional order control strategy. Journal of Intelligent Procedures in Electrical Technology, 4(16):17-28.

[33] Chapman, J. W., Ilic, M. D., King, C. A., Eng, L. (1993). Stabilizing a multimachine power system via decentralized feedback linearizing excitation control, IEEE Trans. on Power Systems,8(3): 830-839.

[34] Zhu, C., Zhou, R., Wang, Y. (1998). A new decentralized nonlinear voltage controller for multimachine power systems, IEEE Trans. on Power Systems, 13(1): 211-216.

[35] Kalyan Kumar, B., Singh, S. N., Srivastava, S. C., A decentralized nonlinear feedback controller with prescribed degree of stability for damping power system oscillations. Electric Power Systems Research, 77(3-4): 204–211.

[36] Guo, Y., Hill, D. J., Wang, Y. (2001). Global transient stability and voltage regulation for power systems, IEEE Trans. on Power Systems, 16(4): 678-688.

[37] Tan, S., Geng, H., Yang, G., Phillips-Heffron model for current-controlled power electronic generation unit. Journal of Modern Power Systems and Clean Energy. 6(3): 582-594.

[38] Wang, H.F., Swift, F.J., (1996). Application of the Phillips-Heffron model in the analysis of the damping torque contribution to power systems by SVC damping control. International Journal of Electrical Power & Energy Systems. 18(5): 307-313.

[39] Padiyar, K. R. (2002). Power system dynamics–stability and control, BS Publications, Hyderabad, India, 2nd edn.

[40] Shahgholian, G., Mohagheghian, E., Mahdavian, M., Farazpey, S., Azadeh, M., Janghorbani, M. (2016). Design of the controller for synchronous generator exciting system by FBL and H_∞ methods, Proceeding of the IEEE/ECTICON, Chiang Mai, Thailand, 1: 1-6.

[41] Gurrala, G., Sen, I. (2011). Synchronizing and damping torques analysis of nonlinear voltage regulators, IEEE Trans. on Power Systems, 26(3): 1186-1195.